ITC FILE COPY

'ORT DOCUMENTATION PAGE

1a	**AD-A209 875**	1b RESTRICTIVE MARKINGS
2a		3 DISTRIBUTION/AVAILABILITY OF REPORT
2b		Appr... for p... release, dist... un... ...d

4 PERFORMING ORGANIZATION REPORT NUMBER(S)	5 MONITORING ORGANIZATION REPORT NUMBER(S)
TM-1352	AFOSR-TR· 89-0825

6a NAME OF PERFORMING ORGANIZATION	6b OFFICE SYMBOL (If applicable)	7a. NAME OF MONITORING ORGANIZATION
CREARE INC.		~~USAF, AFSC~~ AFOSR/NE

6c ADDRESS (City, State, and ZIP Code)	7b. ADDRESS (City, State, and ZIP Code)
ETNA ROAD P.O. BOX 71 HANOVER, NH 03755	BLDG. 410 BOLLING AFB, DC 20332-6448

8a. NAME OF FUNDING/SPONSORING ORGANIZATION	8b. OFFICE SYMBOL (If applicable)	9. PROCUREMENT INSTRUMENT IDENTIFICATION NUMBER
SDIO		F49620-88-C-0137

8c ADDRESS (City, State, and ZIP Code)	10 SOURCE OF FUNDING NUMBERS			
~~SDIO/T/IS~~ BLDG. 410 ~~The Pentagon~~ BAFB ~~Washington, DC 20301-7100~~ 32-6448	PROGRAM ELEMENT NO. 61102F	PROJECT NO. SDI K822	TASK NO. F1	WORK UNIT ACCESSION NO

11 TITLE (Include Security Classification)

SUPERCONDUCTING MEISSNER EFFECT BEARINGS FOR CRYOGENIC TURBOMACHINES

12 PERSONAL AUTHOR(S)

VICTOR IANNELLO, JEFFREY S. MARSHALL, W. DODD STACY

13a TYPE OF REPORT	13b TIME COVERED	14 DATE OF REPORT (Year, Month, Day)	15. PAGE COUNT
FINAL	FROM 88 Sept. TO 89 Mar	1989 May 18	

16 SUPPLEMENTARY NOTATION

17 COSATI CODES			18. SUBJECT TERMS (Continue on reverse if necessary and identify by block number)
FIELD	GROUP	SUB-GROUP	

19 ABSTRACT (Continue on reverse if necessary and identify by block number)

State-of-the-art miniature expansion turbines and centrifugal compressors used in space-borne sensor cryocoolers employ self-acting gas bearings to achieve high reliability and long operating life. Because these bearings must run at room temperature to achieve adequate stiffness and stability, they result in an avoidable source of heat leak to the process gas, thereby lowering overall cycle efficiency and increasing the system launch weight. In this report, it is shown that the gas bearings can be replaced by Meissner effect bearings fabricated from high temperature superconducting materials. Analyses are presented to predict Meissner bearing performance, and a preliminary design of a miniature expansion incorporating Meissner bearings is conceptualized. Because these bearings operate at a cryogenic temperatures, a substantial reduction in heat leak to the process gas can be achieved. For a typical cryocooler providing 1 watt of cooling at 10 K, a 40% reduction in input cycle power can be achieved by replacing the self-acting gas bearings by Meissner bearings in the cold expansion turbine.

20 DISTRIBUTION/AVAILABILITY OF ABSTRACT	21. ABSTRACT SECURITY CLASSIFICATION
☐ UNCLASSIFIED/UNLIMITED ☐ SAME AS RPT. ☐ DTIC USERS	UNCLASSIFIED
22a NAME OF RESPONSIBLE INDIVIDUAL WEINSTOCK	22b. TELEPHONE (Include Area Code) (202) 767-4933 22c. OFFICE SYMBOL NE

DD FORM 1473, 84 MAR 83 APR edition may be used until exhausted. All other editions are obsolete.

SECURITY CLASSIFICATION OF THIS PAGE
UNCLASSIFIED

Creare

SUPERCONDUCTING MEISSNER EFFECT
BEARINGS FOR CRYOGENIC TURBOMACHINES

PHASE I FINAL REPORT

CONTRACT NO. F49620-88-C-0137

Victor Iannello
Jeffrey S. Marshall
W. Dodd Stacy

Project No. 6760
TM-1352
MAY, 1989

CREARE INC.
HANOVER, NH 03755

Executive Summary

This project has looked at the feasibility of an innovative, miniature turboexpander for a spaceborne cryocooler. The innovation lies in the superconducting journal bearings it employs for suspension of the rotating shaft, which generate their load capacity from the Meissner effect.

The incorporation of Meissner bearings into miniature cryogenic turbomachines is a near term application of high temperature superconducting materials. This application is logical because the cold temperatures required by the superconductor need not be artificially created by external cooling, but result from normal operation of the turboexpander. Current turboexpanders employ gas bearings which must be run at room temperature, thereby necessitating a large temperature gradient in the shaft with a corresponding performance penalty due to heat leak into the process gas. By replacing the room temperature gas bearings with cryogenic Meissner bearings, a 40% decrease in input power is attainable for a 1 watt cryocooler that provides cooling at 10 K.

In Phase I we analytically demonstrated the feasibility of the incorporation of Meissner bearings into miniature turboexpanders. We conclude that the stiffness and damping produced by the bearing is sufficient for satellite applications by using superconductor materials in readily–available bulk geometrics. This report documents the methods and results of this assessment.

Based on the strength of our Phase I results, we have high confidence that a successful prototype turboexpander can be designed, built, and tested in Phase II. We therefore advocate continue development of Meissner bearings for cryogenic turbomachine.

Creare

LICENSE RIGHTS LEGEND
Contract No. F49620–88–C–0137
Contractor: Creare Incorporated

Greare

TABLE OF CONTENTS

Greare

LIST OF FIGURES

Greare

LIST OF TABLES

1 INTRODUCTION

1.1 Background

Spaceborne infrared sensors for surveillance and intelligence require cryogenic cooling to achieve high sensitivity levels and signal to noise ratios. The importance of this data demands very high reliability of the cryogenic cooling system. Extended missions further require long cooling system operational lifetime. Additionally, the launch weight of the cryogenic cooling system directly impacts the cost per bit of intelligence data.

Cooling systems which rely upon boil off of liquid or solid cryogens from a dewar provide very high reliability and availability. Launch weight however is directly proportional to mission life in such systems, implying practical limits upon the useful life of spacecraft so equipped. Closed cycle mechanical cryocoolers are currently under development to provide reliable cooling for mission lengths beyond the practical limits of cryogen boil off (open) systems. Two state-of-the-art cryocoolers are currently under advanced development and demonstration, both employing hydrodynamic gas bearings for reliability and long life and both employing the reverse Brayton thermodynamic cycle. Creare has actively participated in one of these two development programs, providing the coldest stage turboexpander for the three stage turbo-based system. Creare is also currently working on several other component and system development projects, such as a 5 watt, 80 K single-stage cryocooler for NASA.

Cryocooler systems based on gas bearing turbomachines appear to have life and reliability issues well in hand, with reliability subject only to well established electronic system design and QA techniques. The key remaining issue concerns system efficiency, that is the cryocooler input power requirement per watt of refrigeration capacity at cryogenic temperatures. The input power requirement and waste heat radiator requirement strongly impact the system launch weight per unit of cooling capacity. All heat which conducts, or "leaks", to the cold end of the system must be lifted by the cryocooler to radiator temperature for ultimate rejection. Each watt of heat leak penalizes the system with many additional watts of input power requirement, a situation of escalating severity as sensor temperatures are lowered.

Gas bearings employed in state–of–the–art cryocoolers need to run relatively warm, since their load bearing capacity relies upon temperature–dependent gas viscosity. Every effort is therefore made in design to minimize the thermal conduction between the warm bearing zone and the cold expansion turbine. Small diameter turbine shafts are overhung as far as possible while still retaining adequately high critical speeds. Structural connections between the warm and cold ends are made as long and thin as possible while still retaining adequate structural stiffness and strength to resist launch loads. Nevertheless, the relative significance of heat leak varies inversely with machine size (cooling capacity), with the practical lower size limit for current machines occurring in the range of 3 – 5 watts.

Magnetic bearings, which do not rely upon temperature–dependent gas properties, promise significant improvements in small system efficiency by virtue of running the bearings cold and reducing or eliminating the heat leak discussed above. Actively controlled magnetic bearings are currently in advanced stages of development and demonstration for both reciprocating and rotary cryogenic turbomachines. Creare, for example, is developing a 14 kW cold centrifugal compressor with active magnetic bearings. Each bearing employs four actively modulated radial electromagnets to suspend the shaft free of contact with its surroundings while providing very high bearing stiffness. Four position sensors continuously monitor shaft position and provide feedback to fast and sophisticated electronic control circuits which in turn actively modulate the bearing magnets. Reliability of this and similar systems is limited only by the reliability of electronic components in the sensing and control circuits.

Passive magnetic bearings employing permanent magnets have also been applied as an alternate and simpler approach to achieving utter reliability. Creare, for example, successfully employs a passive magnetic thrust bearing, in conjunction with self–acting hydrodynamic gas journal bearings, in a line of commercial centrifugal machines for the scientific research community. Unfortunately, as demonstrated by Ernshaw early in the century, it is not possible to fashion a bearing system stable in all three dimensions using just permanent magnets and normal materials.

1.2   Meissner Bearing Description

One of the first observed properties of superconductors is their ability to screen out some or all of the magnetic flux applied by an external source magnet. In the limit of total

Creare

flux exclusion, the superconductor behaves as a perfect diamagnetic material, i.e., a material with magnetic susceptibility given by $\chi = -1$. The exclusion of flux from a superconductor is known as the Meissner effect. The magnetic force on a diamagnetic body is in the direction opposite to the magnetic field gradient, and hence there is a repulsive force developed between a magnet and a superconductor. This is the force responsible for levitating magnets above superconductor disks in simple laboratory displays of superconductivity.

In Phase I, we analytically evaluated whether this repulsive force could be used to levitate the shaft of a miniature cryogenic turbomachine suited to a state of the art sensor cryocooler system. Figure 1.1 schematically shows a configuration for a Meissner bearing. A magnetic shaft (which can be achieved by placing a permanent magnet within an ordinary non–magnetic hollow cylinder) is supported in a superconducting annulus. As the shaft is radially displaced away from the axis of symmetry of the superconductor, a repulsive restoring force is generated. Hence, such a configuration has a finite stiffness associated with it.

The magnetic flux lines in Figure 1.1 are shown penetrating the superconductor. We will show in Section 2 that it is preferable to operate the bearing under conditions in which flux penetration occurs. We designate this partial flux exclusion as Type II behavior, as opposed to Type I behavior which is characterized by total flux exclusion. Although technically the Meissner effect refers to Type I behavior, which is characterized by total flux exclusion, we will continue to refer to our concept as Meissner bearings whether the superconductor is in fact operating as a Type I or Type II superconductor.
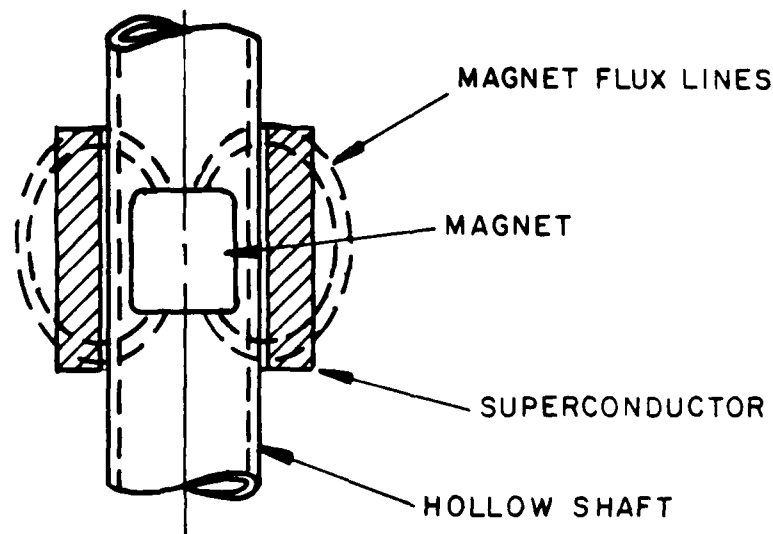
Figure 1.1. SCHEMATIC OF MEISSNER BEARING

3

1.3   Phase I Technical Objectives

The overall technical objective of Phase I was to establish the viability of using the Meissner effect of superconducting materials to provide stable passive magnetic levitation of a high speed rotating shaft. Key issues regarding Meissner effect bearings were: dynamic performance, superconducting material fabrication, and applicability to small turboexpanders used in cryocoolers for spaceborne surveillance sensors. The specific technical objectives as stated in the Phase I proposal are:

1.   Determine the performance characteristics of Meissner effect journal bearings. Particular questions addressed were:

- What are the practical limits of bearing stiffness?

- How much damping is inherent or can be provided?

- How does the bearing stiffness and stability depend on bearing geometry and properties of the superconducting material?

- How does the bearing performance scale with size?

2.   Establish suitable candidates and fabrication means for superconducting materials. Particular questions addressed were:

- What are the relevant superconducting properties of candidate materials: i.e., critical temperature, limits to the Meissner effect.

- What are the means to fabricate the superconducting material to suitable shapes? Is traditional machining possible? Are shapes such as tapes and wires required to assemble an appropriate bearing? What is the potential of application of thin coating or sintering to final shape?

3.   Based on the results of (1) and (2) above, design a Meissner effect bearing for a turbomachine representative of those used in cryocoolers for spaceborne surveillance sensors. Particular questions addressed were:

- What tradeoffs are involved in incorporating a Meissner effect bearing in a cryogenic turbomachine?

- How will the Meissner effect bearing impact the thermodynamic performance and the operating conditions (e.g., start/stop procedures) of the cryocooler?

As described in the sections that follow, all the technical objectives were successfully met. In order to meet these objectives, a 5 task workplan was completed, which is described next.

Greare

1.4 Technical Approach

The workplan for Phase I was organized into the following five tasks:

1. Analysis of Meissner effect bearing performance.

2. Assessment of superconducting materials.

3. Preliminary design of Meissner effect bearings.

4. Assessment of technical viability in spaceborne cryogenic turbomachine applications.

5. Management and reporting.

The results from the first four tasks described in detail in the next four chapters of this report. This report is the final documentation required under Task 5.

1.5 Summary of Phase I Results

A bearing stiffness of 50 N/m can be obtained with YBaCuO in a 0.318 cm diameter shaft size turboexpander. This stiffness is adequate to provide non contact suspension, with normal turbine blade tip clearance, under all loading scenarios typical of the satellite operating environment. Damping adequate to pass through the first (bearing) critical speed can be easily provided by external conductors, and may be inherent in superconductor material flux pinning and hysteretic behavior.

Commercially available bulk YBaCuO has adequate diamagnetic properties to provide the bearing performance described above. Mechanical properties are adequate to sustain stresses and loads associated with cryoexpander applications without cracking or failure. Current molding and sintering fabrication techniques provide adequate dimensional precision without final machining. Material properties are expected to be stable in the inert helium working gas environment.

A Meissner bearing cold stage expander can trim power, radiator size, and weight of a 1 W 10 K cryocooler system by 40%. No significant issues prevent integration of Meissner bearings into such a system. Preventing shaft rotation when the bearings are normal (non

Greare

superconducting) and providing initial cooldown of the bearings during system startup are straightforward.

A Phase II experimental prototype demonstration is expected to be successful.

Greare

2   MEISSNER BEARING PERFORMANCE

Journal bearing performance is typically characterized by the bearing stiffness and damping. Bearing stiffness denotes the radial restoring force imparted to the shaft by the bearing per unit deflection of the shaft from its geometric axis. High bearing stiffness is desirable in order to maintain accurate shaft positioning when loads are applied to the shaft. This is necessary in order to maintain tight turbine blade tip running clearance, which minimizes tip leakage and therefore promotes high aerodynamic efficiency. Damping refers to the dissipation induced by the radial motion of the shaft. Since the shaft and bearing can be thought of as a spring–mass system, damping is necessary for stable rotation of the shaft at speeds at or near the resonant frequency of the bearing–shaft system. The resonant frequency of the bearing–shaft system is known as the "critical speed" of the bearings. Since shaft imbalance (which is to some degree always present) will act as a forcing function to the bearing–shaft system at a frequency corresponding the rotational speed, sufficient damping must be present to "pass through" the critical speed of the bearings, during startup.

In order to analytically derive general expressions for the stiffness and damping produced by Meissner bearings, we consider a generalized geometry, corresponding to a magnet located in a rotating shaft. The stiffness is derived as a function of magnet strength, geometry, and material properties of the superconductor.

2.1   Type I and Type II Superconductors

Materials that exhibit superconductivity at low temperatures are classified as either Type I or Type II. Type I superconductors are typically pure metals such as mercury or lead, and exhibit totally flux exclusion for applied magnetic fields less than some critical field H_c. For fields stronger than H_c, the Type I superconductor loses its superconductivity.

Type II superconductors, which are generally compounds or alloys, exhibit two critical field strengths, denoted H_{c1} and H_{c2}. For field strengths less than H_{c1}, a Type II superconductor will exhibit total flux exclusion, and hence this is referred to as operating the superconductor in the Type I region. For $H_{c1} < H < H_{c2}$, however, Type II superconductors exhibit partial flux exclusion. Superconductivity is lost when H exceeds H_{c2}. A comparison of

7

Creare

Type I and II superconductors is shown in Figure 2.1, which shows perfect diamagnetism (H = − M) exhibited for both types of superconductors for low external fields, and partial flux exclusion for Type II superconductors for $H_{c1} < H < H_{c2}$. For the high temperature superconductors in which we are interested, H_{c1} is quite low ($\sim 10^4$ A/m) and H_{c2} is quite high ($\sim 10^7$ A/m).

2.2   Literature Review of Levitation Forces in Superconductors

The recent discovery of high temperature superconducting ceramic materials has brought renewed interest in levitation forces produced when magnetic fields are applied to superconductors. In fact, this is the effect frequently demonstrated by researchers when a small permanent magnet is levitated above a sample of ceramic superconductor that is cooled in a dish of liquid nitrogen. Early researchers were concerned with levitation forces for Type I superconductors. For example, Simon (1953) presented a two–coil configuration for levitation of a lead sphere, and Harding (1961) succeeded in analyzing the levitation forces used to fabricate a cryogenic gyroscope. In a later study, Rivetti (1987) used Meissner bearings to develop a turbine flowmeter for liquid helium.

With the advent of new high T_c superconductors with relatively small values of H_{c1}, researchers have begun to investigate the levitation forces produced by Type II superconductors. Hellman et al. (1988) studied the levitation of a Nd–Fe–B magnet above a disk of YBaCuO superconductor. They developed a model to predict these forces based on the energy associated with flux penetration in the Type II region. They also concluded that flux pinning forces were responsible for stable levitation since Meissner (Type I) forces alone would not allow stable levitation over a flat disk. Harter et al. (1988) studied the levitation forces produced by a thallium–based superconductor in the Type II region. Their experimental results were in approximate agreement with Hellman et al.'s analyses. They also observed levitation of superconducting samples below permanent magnets, which they attributed to flux pinning forces. Williams and Matey (1988) also observe that flux pinning forces may contribute to the overall stiffness of the system. Moon et al. (1988) observe that the levitation forces are hysteretic in nature, and attributed the hysteresis to flux pinning. This is important for our application because the hysteresis will contribute to the damping for our bearing. Marshall et al. (1989) also observed magnetic hysteresis in the Type II region.
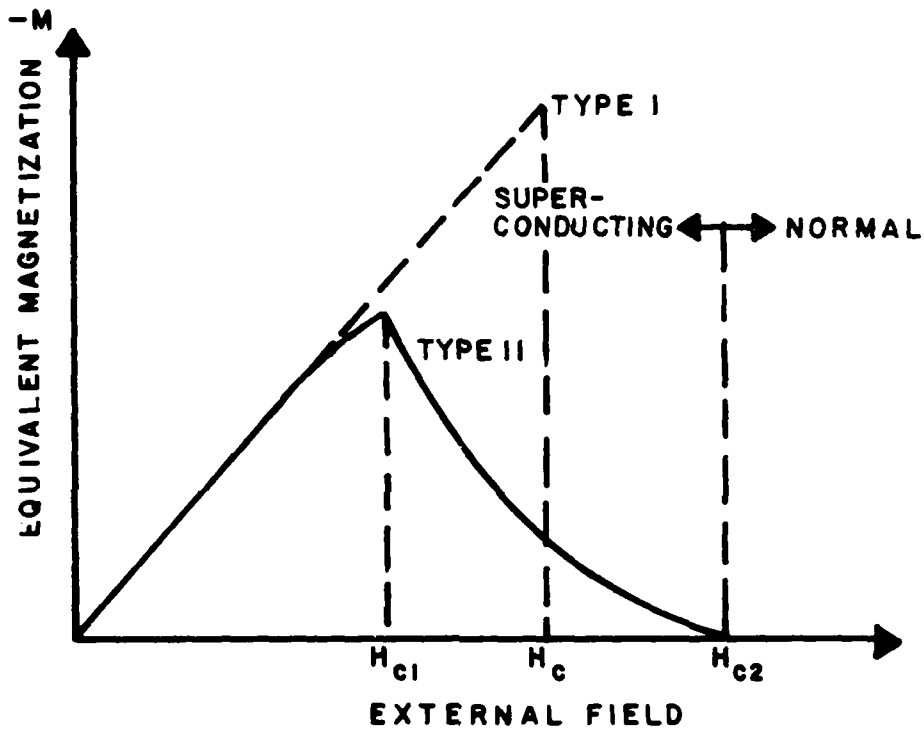
8

Figure 2.1.   COMPARISON OF MAGNETIZATION VERSUS EXTERNAL FIELD FOR TYPE I AND
TYPE II SUPERCONDUCTORS

Based on our literature review, we conclude that Hellman et al.'s model is the state–of–the–art method for predicting levitation forces for Type II superconductors. We will extend this analysis to bearing geometries in Section 2.4.

2.3   Levitation of a Type I Superconductor

The Meissner effect is a well–studied phenomenon in the field of superconductivity. Stated simply, a Type I superconductor will exclude from all but a thin layer near the conductor surface. The screening of the magnetic field from the interior of the superconductor is accomplished by persistent currents that flow at the surface of the superconductor. In fact, the Meissner force physically results from the Lorentz force JxB acting on these persistent currents.

The Meissner effect can be thought of in terms of magnetization fields in the superconductor as follows. For a material with applied field H, the induced field B within the material is given by

$$B = \mu_o \, (H + M) \qquad\qquad (2–1)$$

Since $B = 0$ in the superconductor, $M = -H$, which is valid for Type I superconductors and Type II superconductors operating in the Type I region.

Since the magnetization is maximized for $H = H_{c1}$, it was generally thought that the levitation forces would be maximized for superconductors in the Type I (complete flux exclusion) region, and therefore the levitation of Type I superconductors has been extensively studied analytically and experimentally (eg., Simon, 1952). Hellman et al. (1988) recently showed, both theoretically and experimentally, that levitation can be achieved for Type II superconductors. In fact, by removing the constraint that $H < H_{c1}$, greater forces can be developed by operating in the Type II region. The maximum magnetic pressure developed on the surface of the superconductor in Type I region is given by $\mu_o H_{c1}^2/2$. For the new high T_c compounds, $B_{c1} = \mu_o H_{c1}$ is about 0.01 T (100 G), so that a bearing fabricated from this material operating in the Type I region will generate a maximum pressure of about 40 Pa ($5.9 \cdot 10^{-3}$ psi). Since it is impractical to consider a bearing with such low load capacity, we will only consider superconductors in the Type II region.

10

Creare

2.4 Levitation of a Type II Superconductor

As stated in Section 2.1, for superconductors operating in the Type II region, there is partial penetration of the applied field into the superconductor. One of the fundamental properties of a superconductor is that the flux penetrates in discrete flux bundles called fluxoids. The flux value associated with a fluxoid is $\phi_o = 2.07 \times 10^{-15}$ Wb, which is one–half the ratio of Planck's constant and the electron charge.

Hellman et al. (1988) recently derived an expression for the forces between a magnet and a superconductor in the Type II region by considering the energy necessary for the fluxoids to penetrate the superconductor. Their assumptions were:

- The superconductor does not distort the field produced by the magnet. For a material with sufficiently strong flux pinning, the field would be excluded from the interior of much of the superconductor and therefore the field lines of the magnet would be distorted. However, since we are interested in high temperature superconductors with low values of J_c, the pinning forces are low, and the flux will penetrate the interior in the Type II region.

- The fluxoids do not interact. As long as H << H_{c2}, the fluxoids can be analyzed as independent entities. Since superconductors typically have values of H_{c2} much larger than can be produced by any known magnetic material, this assumption is also valid.

- The fluxoids penetrate straight through the superconductor. The magnetic field produced by a magnet is shown in Figure 2.2. For a sufficiently thin superconductor, field lines will penetrate through the superconductor with very few actually closing within the superconductor. As long as the superconductor thickness is comparable to the size of the magnet (or smaller), this assumption is approximately valid.
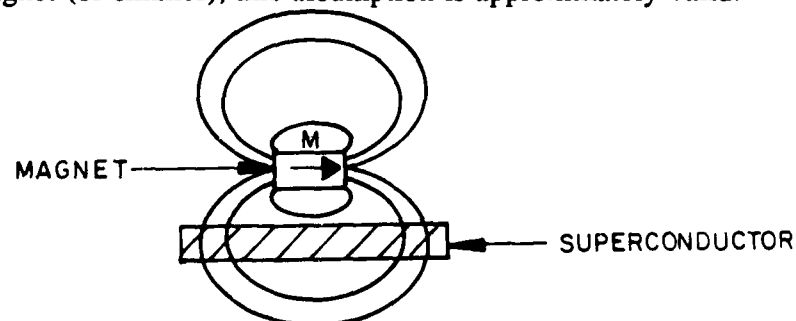

Figure 2.2. FIELD FROM A PERMANENT MAGNET THROUGH A TYPE II SUPERCONDUCTOR

⚙reare

- The magnet is considered to be a point dipole with strength MV, where M is its magnetization, and V is its volume. Since we are concerned with calculating the field outside of the magnet, this assumption is valid to the first-order.

Hellman et al. derived the energy associated with flux ϕ passing through a superconductor of thickness t as follows. Since the total flux must be divided between N fluxoids each containing a flux quantum ϕ_o, the number of fluxoids is $N = \phi/\phi_o$. According to Tinkham (1975), each fluxoid has an energy given by

$$E_o = B_{c1}\phi_o t/\mu_o \qquad (2\text{--}2)$$

so that the total energy associated with putting the fluxoids through the superconductor is

$$E = NE_o = B_{c1}\phi t/\mu_o \qquad (2\text{--}3)$$

The force on the superconductor is then obtained from $F = \Delta E$. Since B_{c1}, t, and μ_o are constant, the force in the x_i direction is given by

$$F = -B_{c1}t/\mu_o \frac{\partial\phi}{\partial x_i} \qquad (2\text{--}4)$$

Hellman et al. used this result to derive the force on a magnet levitated above a flat superconductor of infinite extent, where the magnetic moment of the magnet is parallel to the superconductor surface.

In the next section we will extend Hellman et al.'s analysis to the geometry of interest to us, i.e., the cylindrical bearing geometry. We will consider the magnet as part of the shaft so that the levitation forces imparted on the magnet will also be the restoring force on the shaft. The rotating component of the bearing will be referred to as the rotor, and the stationary part as the stator, which is the nomenclature used for other types of rotating electromagnetic devices.

2.5 Analysis of Cylindrical Bearing with Magnet in Rotor

We first consider the bearing geometry shown in Figure 2.3, which consists of a cylindrical magnet of radius R placed within a shaft. The distance from the center of the
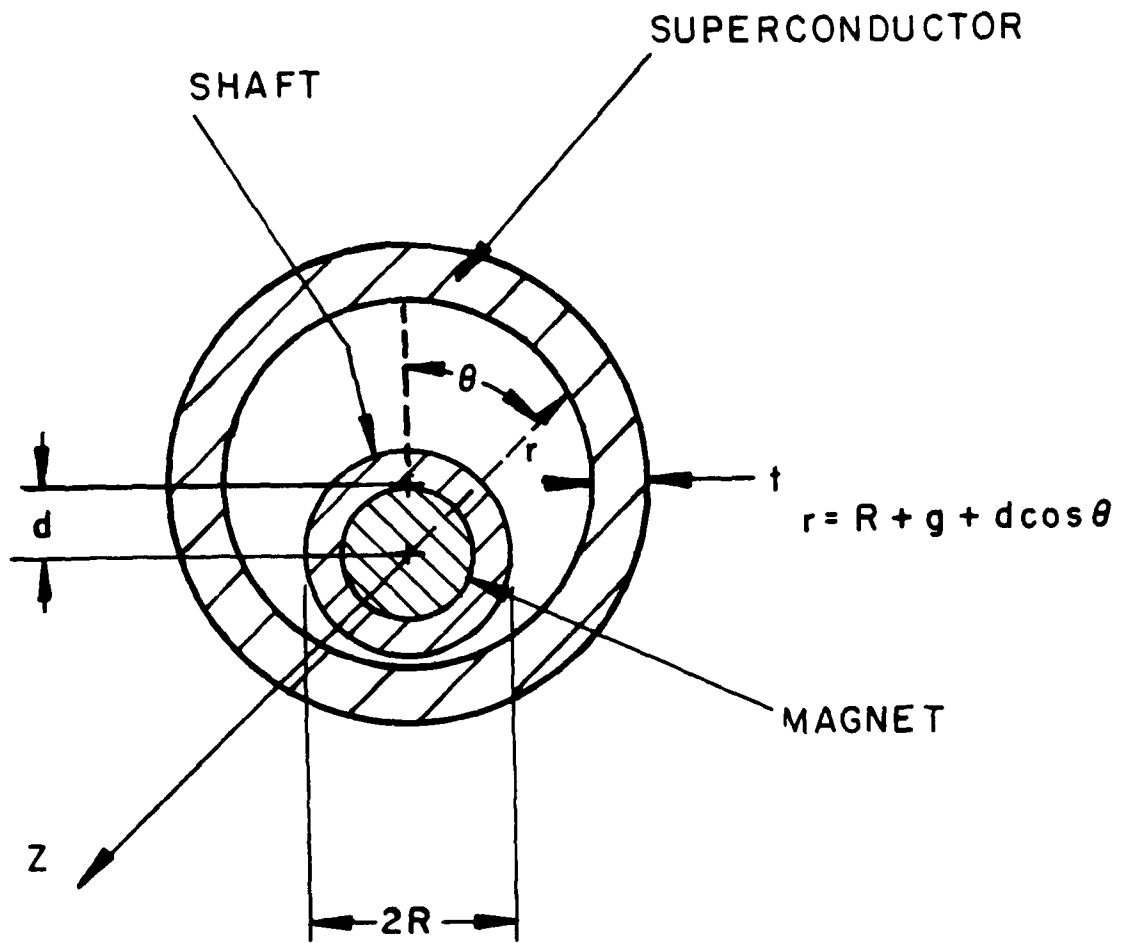
Figure 2.3. MEISSNER BEARING GEOMETRY

magnet to the surface of the superconductor is $r = R + g + d\cos\theta$, where g is the distance between the magnet and superconducting surface assuming no eccentricity, and d is the shaft displacement from the superconducting surface corresponding to angular position θ. The axial position as referenced to the center of the magnet is denoted by z. By symmetry, there will be no force acting on the magnet for d = 0; however, when the shaft is radially displaced (d ≠ 0), there will be a restoring force on the shaft. We wish to calculate the bearing stiffness of such a configuration.

For a spherical dipole of magnetization M aligned with the z–axis, the radial component of the field is given by

$$B_r = \frac{\mu_o M R^3 r z}{(r^2 + z^2)^{5/2}} \tag{2-5}$$

Since the flux through the superconductor for z < 0 will be identical to the flux for z > 0, but of opposite sign, the total flux through the superconductor is given by

$$\phi = 2 \int_0^{2\pi} \int_0^\infty B_r \, dz \, r d\theta \tag{2-6}$$

After substituting (2–5) into (2–6) and performing the integration with respect to z, we find that the flux through a surface strip of width $rd\theta$ extending from $z = -\infty$ to $z = \infty$ is given by

$$d\phi = \frac{2\mu_o M R^3}{3\,r} d\theta \tag{2-7}$$

From (2–3), the fluxoid energy associated with this flux is

$$dE = \frac{2 B_{c1} M R^3}{3r\,t} d\theta \tag{2-8}$$

From (2–4), the radial component of the force on the magnet due to this strip is

$$dF = \frac{2 B_{c1} M R^3}{3r^2\,t} d\theta \tag{2-9}$$

14

Creare

In order to calculate the net force on the shaft, it is necessary to integrate (2–9) for all θ, recognizing that the component of the force in the direction of the displacement is given by dFcosθ. Thus the restoring force on the shaft is

$$F = \frac{2}{3}B_{c1}MR^3/t \int_0^{2\pi} \frac{\cos\theta}{r^2} d\theta \qquad (2-10)$$

For small displacements, $1/r^2$ can be linearized to

$$\frac{1}{r^2} = \frac{1}{(R+g+d\cos\theta)^2} \simeq \frac{1}{(R+g)^2} - \frac{2b\cos\theta}{(R+g)^3} \qquad (2-11)$$

After substituting (2–11) into (2–10) and simplifying, the restoring force on the shaft is calculated to be

$$F = -\frac{4}{3}\pi b B_{c1}Mt \left[\frac{R}{R+g} \right]^3 \qquad (2-12)$$

The stiffness, which is defined as $K = -dF/dd$, is thus

$$K = \frac{4}{3}\pi B_{c1}Mt \left[\frac{R}{R+g} \right]^3 \qquad (2-13)$$

Figure 2.4 plots bearing stiffness versus M for various B_{c1} values for small gaps relative to the size of the magnet. For our application, we are interested in levitating shafts approximately 0.318 cm (1/8 in) in diameter. For a neodymium rare–earth magnet levitated above a YBaCuO superconductor, we can assume a magnetization field $\mu_o M = 0.5$ T and a lower critical field $B_{c1} = 0.01$ T. Assuming the superconductor thickness t is equal to the shaft diameter, a stiffness of about 53 N/m is predicted per bearing.

2.6 Damping Requirements

In this section, we will discuss the stability of the bearing with shaft excitations, and particularly focus on the damping of these excitations near the resonance point. The excitation of the shaft may arise either internally from shaft imbalance or may be externally imposed.
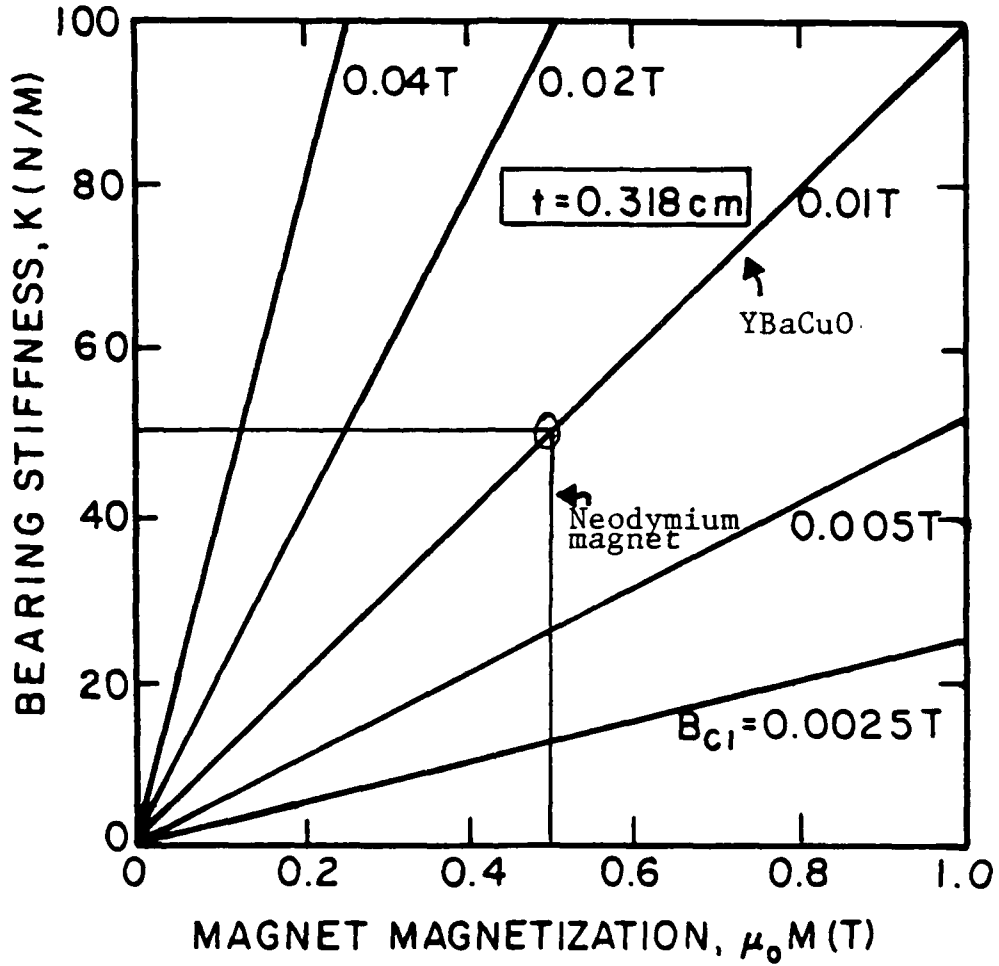
Figure 2.4. MEISSNER BEARING STIFFNESS VERSUS MAGNET STRENGTH FOR SMALL GAP RELATIVE TO MAGNET SIZE

Creare

Similarly, the damping may arise either internally due to viscous aerodynamic and other forces, or it may be externally imposed. The latter type of damping is referred to here as "controlled", since it can be adjusted so that the desired amount of damping is achieved.

The displacement of the shaft from its equilibrium location is governed by the equation

$$m \ddot{d} + b\dot{d} + Kd = F_o [\sin(\omega t) + \cos(\omega t)] \tag{2-14}$$

where a superposed dot denotes differentiation with respect to time, and where m is one–half the shaft mass (assuming a two–bearing system), b is the damping coefficient, K is the stiffness introduced in Section 2.2 and F_o is the magnitude of the shaft excitation force with frequency ω. We assume in this section that the shaft excitation is due entirely to shaft imbalance (the effect of environmental vibrations is discussed in Section 5.1), and so F_o is given by

$$F_o = \varepsilon \, m \, \omega^2 \tag{2-15}$$

where ε is the shaft imbalance.

The solution of (2.3.1) is given by

$$d = F_o \left[\frac{b\omega - \omega^2 M + K}{(b\omega)^2 + (K - \omega^2 m)^2} \right] \sin(\omega t) + F_o \left[\frac{-b\omega - \omega^2 m + K}{(b\omega)^2 + (K - \omega^2 m)^2} \right] \cos(\omega t) \tag{2-16}$$

We notice that if b = 0, then d becomes unbounded when ω approaches the shaft natural frequency ω_n, given by

$$\omega_n = (K/m)^{1/2} \tag{2-17}$$

It is convenient at this point to define the damping ratio ζ by

$$\zeta = \frac{b}{2 \, m\omega_n} \tag{2-18}$$

17

ⓢreare

The maximum value of d, denoted by d_{max}, occurs when ω equals the resonant frequency ω_n, and from (2–15) – (2–18) it can be shown that

$$d_{max} = \frac{\varepsilon}{2\zeta} \qquad (2\text{–}19)$$

A plot showing the variation of d_{max} with ζ for various values of ε is given in Figure 2.5. A typical value of ε for the proposed application is 0.5 μm (20 μ inch). We require d_{max} to be less than about half of the turbine blade tip running clearance (which is much smaller than the planned bearing gap width), or about 25 μm (0.001 in). The minimum required damping ratio for the bearing is then obtained from (2.3.6) as

$$\zeta_{min} = 0.01 \qquad (2\text{–}20)$$

although we will design for ζ somewhat greater than ζ_{min}.

2.7 Controlled Damping

The controlled damping can be provided by coils placed outside of the superconducting layer and opposite to the north and south magnetic poles. A diagram illustrating the operation of the controlled damping loops is given in Figure 2.6. As the shaft shifts to the left in the figure, the magnitude of the magnetic field in the loops on the left increases and that of the loops on the right decreases, and these changes set up electrical currents in the coils. The loops are made of highly conductive material in order to maximize the currents, and hence the rate of energy dissipation, within the loops. The energy loss in the loops is extracted from the excitation energy of the shaft, hence providing a net damping force on the bearing.

For a coil of N turns experiencing a time varying field, we find that the emf E set up in the coil is

$$E = N\dot{\phi}_c \qquad (2\text{–}21)$$

18
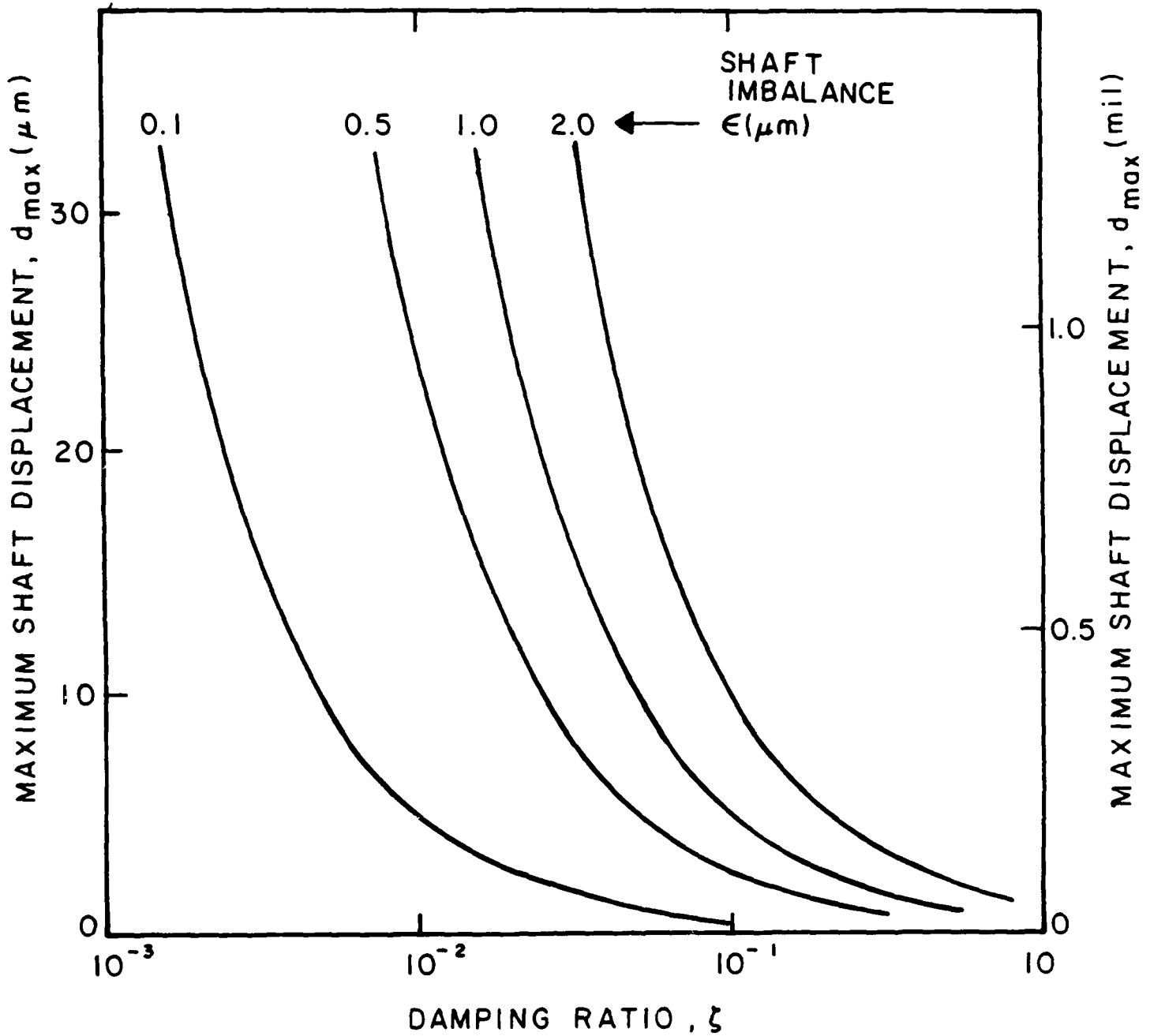
Figure 2.5. MAXIMUM SHAFT DISPLACEMENT AS A FUNCTION OF DAMPING RATIO AND SHAFT IMBALANCE
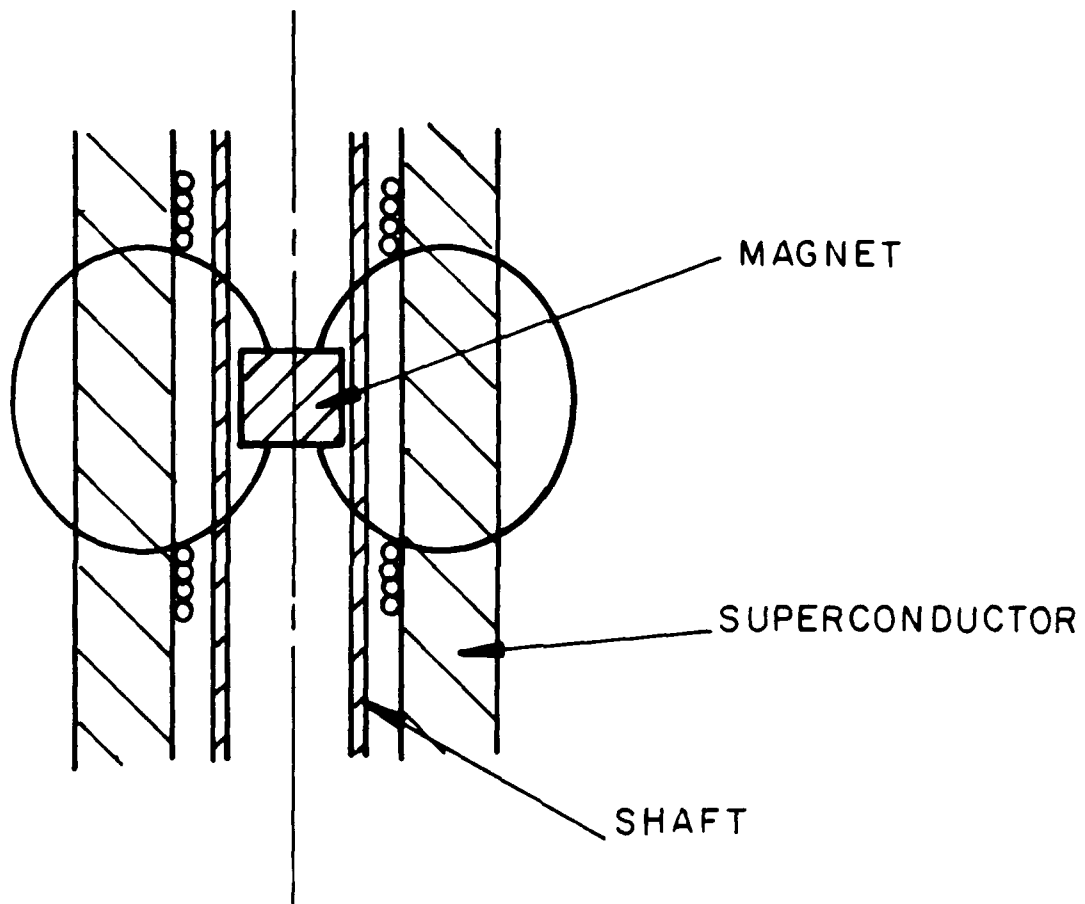
Figure 2.6. ARRANGEMENT OF DAMPING COILS FOR BEARING

where $\dot{\phi}_c$ is the rate of change of the flux passing through the coil. If the resistance of the coil is $\mathbb{R}$, energy is dissipated at a rate

$$P = E^2/\mathbb{R} = N^2\dot{\phi}_c^2/\mathbb{R} \tag{2-22}$$

Assuming that this dissipation can be represented by a damping constant b, the dissipation rate is written

$$P = b \, \dot{d}^2 \tag{2-23}$$

Equating (2-22) and (2-23) and solving for b yields

$$b = N^2(\dot{\phi}_c/\dot{d})^2/ \mathbb{R} \tag{2-24}$$

Next we solve for the flux ϕ_c through the coil as a function of shaft displacement. Assuming each coil encompasses one quadrant of the bushing, the flux is given by (2.7):

$$\phi_c = \int_0^{\pi/2} \frac{2\mu_0 MR^3}{3\,r} d\theta \tag{2-25}$$

where $1/r$ can be linearized to

$$\frac{1}{r} = \frac{1}{R+g+d\cos\theta} \approx \frac{1}{R+g} - \frac{d\cos\theta}{(R+g)^2} \tag{2-26}$$

Substituting (2-26) into (2-25) and integrating yields

$$\phi_c = \frac{2\mu_0 MR^3}{3(R+g)} \left[\frac{\pi}{2} - \frac{d}{R+g} \right] \tag{2-27}$$

The quantity $\dot{\phi}_c/\dot{d}$ is therefore

$$\dot{\phi}_c/\dot{d} = -\frac{2\mu_0 MR^3}{3(R+g)^2} \tag{2-28}$$

ⒼReare

Substituting (2–28) into (2–24) yields a damping constant of

$$b = N^2 \left[\frac{2\mu_o MR^3}{3(R+g)^2} \right]^2 / \mathbb{R} \tag{2–29}$$

Since the two coils that are diametrically opposite will see the same rate of flux change (but opposite sign), the actual damping is twice this value.

Assuming each damping coil is eight turns and has a resistance of about 0.01 Ω, D = 2R = 0.381 cm (1/8 in), and $\mu_o M = 0.5$ T, the damping per coil is 7.2 x 10^{-3} Ns/m. If the bearing has stiffness K = 50 N/m and the shaft mass is 2.5 g, the critical speed of the bearing–shaft system is 32 Hz. From (2–18), the effective damping ratio for a pair of coils would be $\zeta = 0.02$, which exceeds our minimum required value of 0.01. The assumed coil resistance of $\mathbb{R} = 0.01$ Ω is easily attainable for our eight turn coil of copper at cryogenic temperatures. Therefore, we believe that more than adequate damping can be supplied by the coils.

2.8   Other Dissipative Forces

We have demonstrated in the previous section that controlled damping is sufficient to achieve the desired damping ratio, even without including other damping effects, such as fluxoid penetration in the superconductor and hysteresis effects in the permanent magnets, which might additionally contribute to the overall damping of the bearing. Internal damping in the superconductor in particular may substantially contribute to the overall damping of the bearing. For instance, Moon and Raj (1988) operated a superconducting bearing up to speeds of 60,000 rpm, apparently with no damping other than that provided by the superconductor. Internal damping in the superconductor can be explained if we recall (Tinkham, 1975) that each flux vortex can only pass a certain flux quantum. Thus, when the shaft comes closer to the superconducting surface and the magnetic flux at the surface increases, new flux vortices must be formed in the superconductor. The formation of these flux vortices involves a time–varying magnetic field in an ordinary conductor (inside the fluxoid), so that some electrical currents are set up within the fluxoid which dissipate energy. This dissipated energy is drawn from the excitation energy of the bearing, and thus provides damping to the bearing. A quantitative analysis of this effect is somewhat outside the current state of the literature on

superconductivity, and we will not attempt a detailed analysis here since it has already been shown that "controlled" damping is more than sufficient to provide the necessary damping forces on the bearing. In the Phase II Program, however, we will evaluate magnetic damping in the Phase II region to determine if it alone is sufficient for stable spinning of the shaft.

Aerodynamic effects, on the other hand, may either stabilize the bearing and contribute to the damping, or they may destabilize the bearing and promote whirl. The magnitude of the aerodynamic restoring force (calculated from Grassam and Powell, 1964) is plotted in Figure 2.7 for three bearing temperatures at typical design conditions of D = 0.318 cm (1/8 in) and f = 9000 rev/sec. A comparison is also made with the maximum magnetic force for this case obtained from Figure 2.4 with d_{max} = 0.025 mm (0.001 in). We find from Figure 2.7 that at T = 77 K, which is the maximum planned operating temperature, the magnetic force dominates the aerodynamic forces for gap sizes greater than about 0.25 mm (0.010 in). The magnitude of destabilizing aerodynamic forces is very complicated to calculate but is expected to be less than the magnitude of the total stable aerodynamic force. Thus, as long as gap sizes in the bearings are larger than some critical value, in this case about 0.25 mm, we should be justified in neglecting any destabilizing aerodynamic forces.
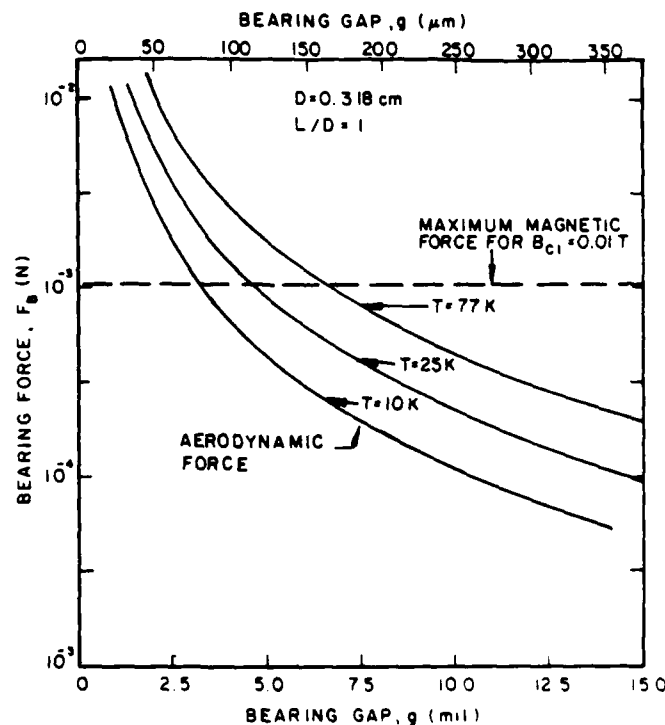

Figure 2.7. AERODYNAMIC FORCE AS A FUNCTION OF BEARING GAP SIZE FOR SEVERAL BEARING TEMPERATURES

Greare

3 MATERIALS ASSESSMENT

In this section, we review the material properties and fabrication issues which are relevant to the proposed Meissner bearing application. Since the desired operating temperatures of the bearing are in the range of liquid nitrogen temperatures, emphasis is placed on the new high temperature superconductors, although one of the older superconducting materials (niobium–tin) will also be included to provide a comparison.

3.1 Material Properties

The material properties are for convenience divided up into two general classes, namely superconductive properties and mechanical properties, and we will discuss these two property types separately. The superconductive properties are summarized in Table 3.1 for five different Type II superconductive materials with critical temperatures ranging from 18 K to 125 K. The superconductive properties of interest for this application include the critical temperature T_c, the lower and upper critical magnetic inductances B_{c1} and B_{c2} evaluated at a typical operating temperature T_{op}, and the flux penetration depth δ. The critical temperature T_c determines the maximum possible operating temperature for each material, but a more realistic operating temperature is about 0.8 T_c. The value of T_{op} in Table 3.1 is selected to be close to 0.8 T_c, but in some cases corresponds with the atmospheric boiling temperature of convenient coolants (see Table 3.2). We note that B_{c1} tends to decrease and B_{c2} tends to increase with T_c for the different materials.

It has been found by several investigators (e.g., Uchida et al., 1987) that the critical magnetic fields vary almost linearly with temperature for high temperature superconducting materials, so we can estimate B_{c1} and B_{c2} for temperatures $T < T_c$ from the values given for T_{op} in Table 3.1 and the relations

$$B_{c1} = B_{c1o} (1 - T/T_c), \quad B_{c2} = B_{c2o} (1 - T/T_c) \tag{3-1}$$

where B_{c1o} and B_{c2o} are the $T = 0$ K values.

Creare

Table 3.1. SUPERCONDUCTIVE PROPERTIES OF VARIOUS TYPE II SUPERCONDUCTORS. B_{c1} AND B_{c2} ARE EVALUATED AT THE SPECIFIED OPERATING TEMPERATURE T_{op}, AND T_c IS EVALUATED IN THE ABSENCE OF MAGNETIC FIELDS AND ELECTRICAL CURRENTS

Material	T_c (K)	B_{c1} at T_{op} (T)	B_{c2} at T_{op} (T)	T_{op} (K)	δ (Å)
NbSn	18[a]	0.12[e]	11[a]	14	400[b]
LaBa(Sr)CuO	35[c]	0.04[c]	12[c]	27	—
YBaCuO	93[d]	0.012[d]	15[d]	77	1500[b]
BiSrCaCuO	103[f]	0.0045[f]	—	77	—
TlBaCaCuO	125[g]	~ 0.004	—	77	—

Sources:
a. Moon et al. (1988)
b. Murphy et al. (1988)
c. Uchida et al. (1987)
d. Kumakura et al. (1987)
e. calculated from data of Murphy et al. (1988) and
   Eq. (3) of Laquer (1988)
f. Kumakura et al. (1988)
g. Lee et al. (1988)

Table 3.2. BOILING TEMPERATURES OF SEVERAL POSSIBLE COOLANTS AT ATMOSPHERIC PRESSURE

Liquid Coolant	Boiling Temperature (K)
Helium	4.2
Hydrogen	20.3
Neon	24.5
Nitrogen	77.4
Argon	87.5

Creare

Based on the results of Section 2, we desire the superconducting material with a value of T_{op} of 75 K or above which has the greatest value of B_{c1}, since the stiffness is proportional to B_{c1} for superconductors with weak flux pinning. (Recall that the hottest turbine in the three–stage cryocooler is usually designed to operate at about 75 K.) From Table 1, that the optimal superconducting material for the proposed bearing application is YBaCuO.

The relevant mechanical properties of YBaCuO at 77 K are listed in Table 3.3 and include mass density, specific heat, thermal conductivity, elastic modulus, thermal expansion coefficient and strain–to–failure. The strain–to–failure is based on usual tensile test measurements and may be different in other geometries. If the superconductive material is placed on the bushing in bulk form, it is found that the internal forces from the fluxoids are far lower than those necessary to crack the material. External forces acting upon the superconducting annulus would tend to put the material in compression, rather than tension, which would also tend to inhibit crack growth.

Table 3.3. MECHANICAL PROPERTIES FOR YBaCuO at 77 K	
Property	**Value at 77 °K+**
density (kg/m^3) [void–free sample]	6380
specific heat (J/kgK)	157
thermal conductivity (W/mK)	13
elastic modulus (GPa)	110
thermal expansion coefficient (1/K)	0.7×10^{-5}
strain–to–failure (%)	$0.1 - 0.2$
+ From Green (1988), with slight modifications.	

It seems that the most likely source of cracking in the superconductive material in the bushing, outside of shaft–bushing contact, would result from non–uniform thermal expansion between the superconductor and the material to which it is bonded. For instance, the thermal expansion coefficient for silver at 300 K is 1.9×10^{-5} 1/K. Silver is one of the few materials with which YBaCuO does not react, so it is a likely choice to which to bond the super-

conductor. The thermal expansion coefficient for YBaCuO at various temperatures is plotted in Figure 3.1. Since the silver shrinks more than the superconductor as the temperature is decreased from its stress–free value, the superconductor undergoes a compressive shearing force along its outer surface. The greatest principal value of strain ε in the superconductor due to this exterior shearing is directed radially inward and is given approximately by

$$\varepsilon = -\nu (\alpha_{silver} - \alpha_{sc}) \Delta T \qquad (3\text{--}2)$$

where Poisson's ratio ν has a typical value of 0.3, α_{silver} and α_{sc} are expansion coefficients for silver and the superconducting material, and ΔT is the temperature change from a stress free state (we assume that ΔT is negative here). For a maximum value of ε at failure of 0.001 and for $\alpha_{silver} - \alpha_{sc} = 6 \times 10^{-6}$ 1/K, we find that the maximum temperature decrease before failure is 500 K. Thus, if the silver is joined to the superconductor at room temperature, e.g., using a friction fit, there should be no problem with cracking of the superconductor material.

3.2 Fabrication Techniques

The results of Section 2 and the earlier parts of this section have indicated that the most promising bearing designs would involve a fairly thick (nominally equal to the shaft diameter) superconducting annulus made of YBaCuO and placed in the bushing with a fairly large (nominally 0.25 mm) gap separating the stationary superconducting surface and the rotating shaft. Possible material fabrication and durability issues involve the following:

(i)   formation of the annulus into its required shape with sufficient precision,

(ii) degradation of the material in the presence of a helium atmosphere and of other metals,

(iii) maintenance or enhancement of superconducting properties of the material, especially material magnetization in the presence of high applied magnetic fields.

Because our bearing performance does not require a small (less then 50 μm) gap between the shaft and the superconductor, fabrication issues regarding precision machining of components is avoided. We have contacted several companies specializing in the manufacture
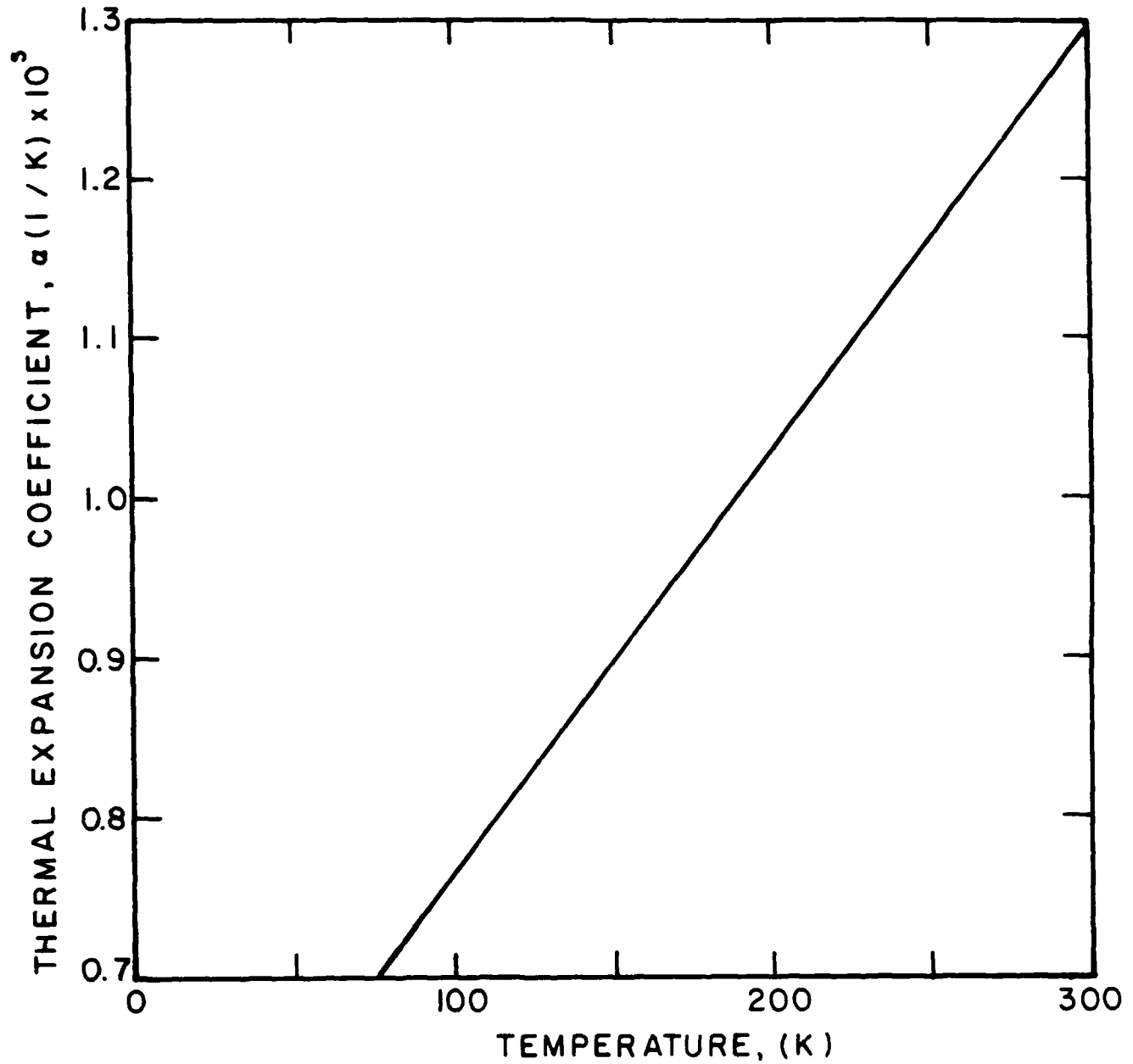
Figure 3.1. THERMAL EXPANSION COEFFICIENT FOR YBaCuO AS A FUNCTION OF TEMPERATURE

Creare

of superconductive materials, and have learned that the annulus described previously can be made fairly easily either by sintering a superconducting cylinder and then machining a hole through its center, or by forming the superconductive material in a mold. (Two companies presently using these techniques are Super Conductive Components Inc. in Columbus, Ohio, and CPS Superconductor, in Cambridge, Mass.) The desired precision (nominally 25 μm) can easily be attained with either technique.

YBaCuO is known to degrade in the presence of oxygen, water, carbon dioxide, common organic materials, and reactive metallic elements. Short–term exposure to air does not seem to greatly affect YBaCuO, but long–term exposure has been found to significantly degrade its superconductive properties. Helium gas is not know to effect YBaCuO, nor would it be expected to since helium is an inert gas. Nonetheless, this will be investigated in Phase II. Also, YBaCuO has been found to be non–reactive with silver. The usual working fluid in our cryogenic turbomachines is helium gas, and we will evaluate using either a silver fitting in the bushing or a silver coating on the non–exposed sides of the superconductive annulus to protect against reactions between the superconductor and other metallic elements in the bearing. A silver coating can also be applied on the shaft if that should prove necessary.

We are therefore confident that high quality superconductive components can be obtained for the bearing and that the superconductive properties of these components can be maintained with no crack development or material degradation throughout the planned bearing life with presently commercially available materials and fabrication techniques.

Creare

4   DESIGN OF TURBOEXPANDER WITH MEISSNER BEARINGS

In this section, we present the design of a turboexpander that incorporates Meissner bearings for its two journal bearings. The design is similar to other turboexpanders we have developed with self—acting journal bearings. Unlike other designs, however, the bearings are fabricated from bulk superconductor and magnets are placed within the shaft.

4.1   Turboexpander Description

A turboexpander utilizes a turbine rotor and a compressor rotor on a single shaft. The turbine rotor extracts power from the cycle gas and thereby provides cooling of the gas. This power is transmitted by the shaft to the compressor rotor, also called a brake fan, which converts the shaft power to compression. The power characteristics of the turbine and brake rotors are suitably matched in order to control the speed of rotation of the shaft.

In our Meissner bearing turboexpander, the power extracted by the turbine provides cooling for the coldest stage of a spaceborne cryocooler. The total cooling requirement of the turboexpander is relatively small — less than 10 W. As a result, the size is very small and the rotational speed of the turbine is very high. Also, the net shaft power transmitted to the brake, potentially available as useful work, is low compared to the cycle input power — about 5 W compared to more than 5 kW, respectively. Recovery of this relatively small amount of power for use elsewhere in the cycle is impractical. It is therefore dissipated as heat in a brake circuit heat exchanger.

A simplified schematic illustrating the operating principle of the turboexpander is shown in Figure 4.1, and an assembly layout of the turboexpander is shown in Figure 4.2. The turboexpander consists of three principal sections. One end contains the brake rotor and operates at approximately 75 K. The turbine is on the other end and operates at temperatures near that of the cold stage load (8 − 15 K). The thermal isolation section connects the warm and cold ends. The thermal isolation section design is a compromise between high structural rigidity and robustness, and low heat conductance from the warm end to the cold end.
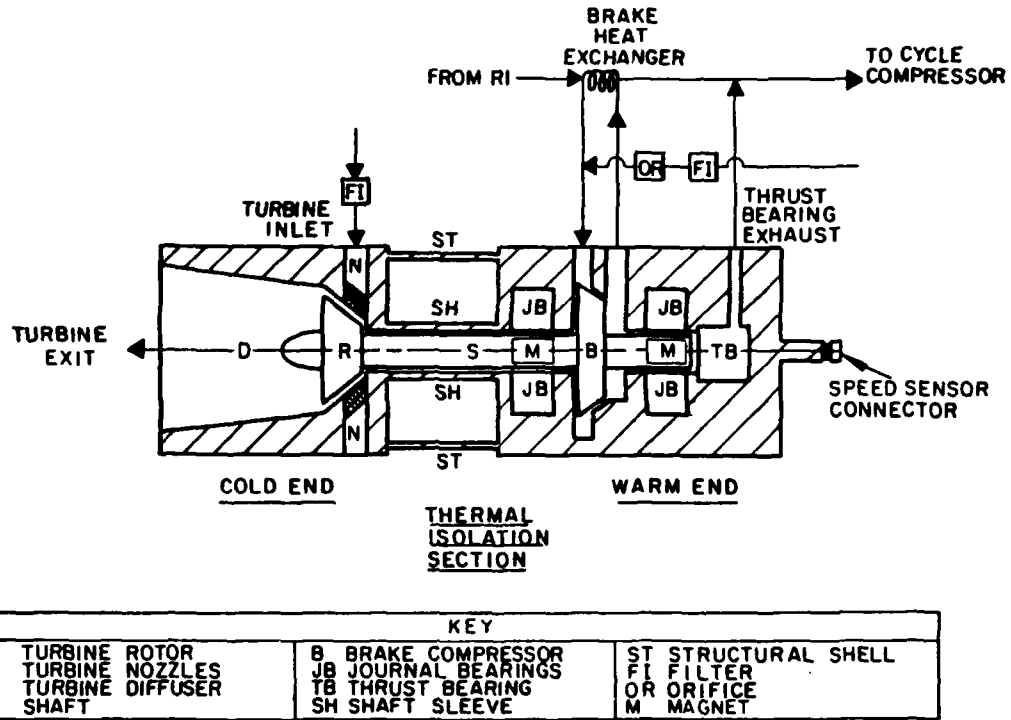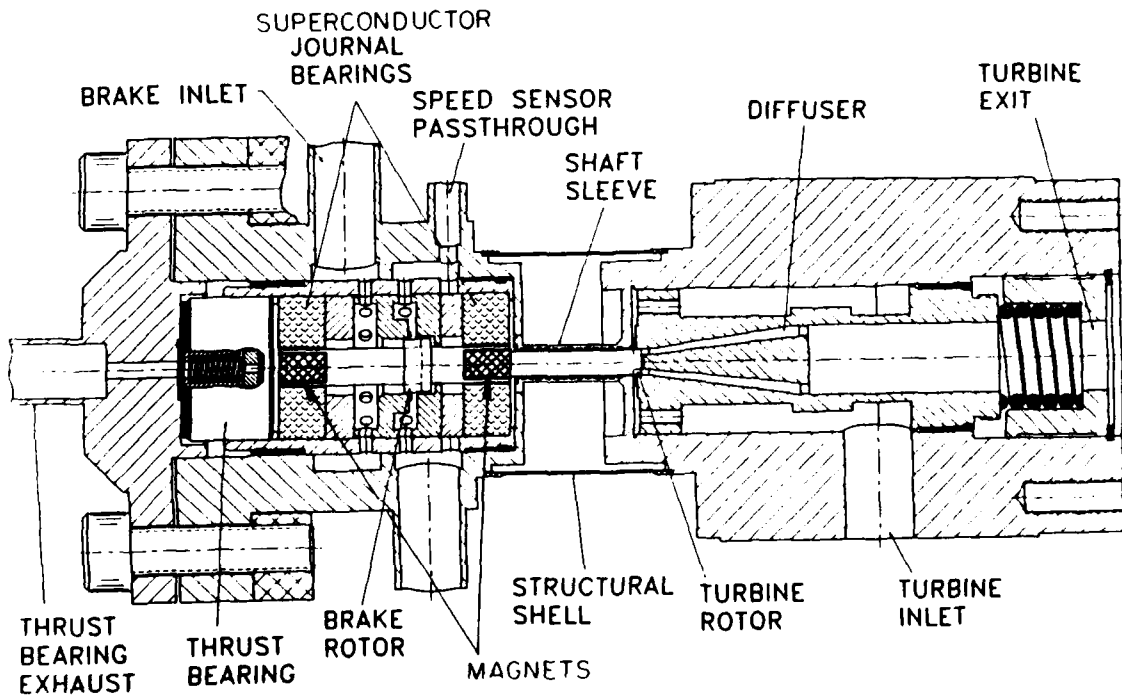
Figure 4.1. TURBOEXPANDER SCHEMATIC

Figure 4.2. TURBOEXPANDER ASSEMBLY LAYOUT

Creare

The expansion of the cycle gas occurs in the cold end of the turboexpander. High pressure gas enters the cold end through the turbine inlet after first passing through a filter. The gas flows through an annular passage to stationary nozzles then through the turbine rotor. As a result of the overall expansion, energy is removed from the cycle gas providing useful refrigeration. This energy extracted from the gas is transmitted by the shaft to the brake wheel in the warm end. The cycle gas leaves the cold end of the turboexpander through a conical diffuser and the turbine exit tube connection to provide cooling at the primary load.

Shaft power from the turbine is absorbed in the warm end by the brake compressor, by drag in the bearings and by windage. The brake wheel circulates helium gas through a brake circuit which consists of flow passages internal to the warm end and external ducting to and from the brake circuit heat exchanger. Gas flow in internal flow passages of the warm end provides convective cooling to remove heat produced by bearing drag and shaft windage. This heat, as well as the energy absorbed by the brake, is rejected from the brake circuit to the warmer first stage of a multistage cryocooler.

The pressurized gas thrust bearing typically requires a flow of 0.1 − 0.5% of the cold turbine flow rate. Supply flow for the thrust bearing originates from the high pressure supply side of a warmer stage turbine, to avoid the efficiency penalty of consuming cold stage gas. An orifice in the thrust supply line is sized such that the supply flow balances the thrust exhaust flow when the brake circuit and warm end pressure equals the cold end turbine rotor inlet pressure. This provides a zero ΔP across the shaft labyrinth, minimizing gas leakage and convective heat leak between the warm and cold ends of the expander. Shaft speed and position are monitored by the speed sensor located in the brake end of the turboexpander.

4.2   Shaft and Bearings Design

The shaft contains the integral turbine rotor, brake rotor, and magnets for the bearings. The shaft is approximately 3.6 cm (1.4 in) long and is fabricated from titanium alloy Ti–6Al–4V. This material has relatively low thermal conductivity while also having a high strength–to–weight ratio at cryogenic temperatures. To reduce the weight of the shaft, it is hollowed along most of its length. Two permanent magnets are inserted at axial locations corresponding to the superconductor journal bearings. The magnets are fabricated from

neodymium rare–earth material because of the high energy products obtainable for these materials. The shaft and bearing design is summarized in the Table 4.1.

Table 4.1. SHAFT AND BEARING DESIGN OF TURBOEXPANDER		
Shaft mass	m	2.5 g
Shaft length	L_s	3.6 cm
Shaft diameter	D	0.318 cm
Journal bearing length	L_b	0.636 cm
Magnet length	L_m	0.318 cm

4.3   Turbine Design

The principal aerodynamic elements of the turbine are the rotor, nozzles and diffuser. The tip diameter of the radial inlet turbine rotor is 0.318 cm (0.125") and the hub diameter is 0.211 cm (0.083"), corresponding to a hub–to–tip diameter ratio of 0.664. There are 11 full blades and 11 splitter blades. The radial inlet turbine blade passages are EDM–machined into the shaft. Rotor geometry, outlet tip angle and hub–to–tip diameter ratio are variable within limits in the EDM process. The turbine nozzles, shroud and exhaust diffuser are machined into a single piece of stock. The conical diffuser has an area ratio of 3.69 with an included half–angle of 3.5 degrees. The turbine rotor, nozzle and diffuser geometry parameters are summarized in Table 4.2.

4.4   Cooldown Circuit

During normal operation of the turboexpander, the cooling provided by the brake circuit heat exchanger ensures that sufficiently cold temperatures are maintained in the superconductor; however, before start up of the machine, there is no circulation of gas in the rake circuit, and therefore no cooling is provided. An alternate cooldown circuit is thus necessary to facilitate safe startup.

Sreare

Table 4.2.	TURBINE ROTOR, NOZZLES AND DIFFUSER PARAMETERS
TURBINE ROTOR	
No. of Blades/Splitters	11/11
Blade Inlet Angle	0°
Blade Exit Angle	17°
Turbine O.D.	0.318 cm
Hub/Tip Ratio	0.664
NOZZLES	
No. of Nozzles	16
Exit Angle	76°
Throat Area	0.0813 mm^2
DIFFUSER	
Area Ratio	3.69
Half Angle	3.5°

The brake circuit is an ideal gas flow path for cooldown because it is in close proximity to both journal bearings. Since the turboexpander bearings in the warmer stages are self-acting gas bearings, the warm stage turbines can be operated to provide cooling to the cold stage turbine Meissner bearings via the brake circuit. The orifice in the thrust bearings supply line can be bypassed through a parallel solenoid valve to provide a higher flow rate of 75 K gas for accelerated cooldown. Gas leakage out the thrust bearing exhaust and down the shaft labyrinth completes the cooldown flow circuit. Once the bearing temperature is below the critical temperature of the superconductor, gas can be introduced to the turbine to start the shaft spinning and to begin to provide cold stage load cooling. In this way, the cryocooler system can "boot strap" itself through startup and cooldown without a need for an external cooling mechanism.

reare

5 ASSESSMENT OF TECHNICAL VIABILITY

In this section, we evaluate the feasibility of using Meissner bearings for the turbo-expander of a spacecraft cryocooler. We focus our evaluation on the 0.318 cm (1/8 in) turboexpander described in Section 1 since it is representative of the turboexpanders we are currently developing for spacecraft cryocoolers.

5.1 Load Capacity and Stiffness

The shaft of the turboexpander will be subjected to external forces which will tend to displace it from its equilibrium position. The bearing system must have sufficient load capacity so that these external forces do not produce contact between rotating and stationary components of the turboexpander. Here we consider the external forces from spacecraft acceleration, gyroscopic effects, spacecraft vibration, and aerodynamic imbalance on the turbine blades.

Spacecraft Acceleration. Once the spacecraft is placed in orbit, it will theoretically be in free fall, and thus the turboexpander will experience a zero gravitational field. Acceleration of the spacecraft may be necessary, however, for orbital maneuvers. For the design stiffness of 50 N/m per bearing, and a shaft mass of 2.5 g, the maximum allowable acceleration is 2.0g. Since spacecraft maneuvering typically requires accelerations of less than 0.1g, the design bearing capacity is more than adequate to accommodate spacecraft accelerations.

Gyroscopic Effect. When a spinning shaft with angular momentum M_s is rotated about another axis with angular frequency Ω, a torque τ is produced on the shaft, which is given by

$$\tau = \Omega \times M_s \qquad (5-1)$$

and is known as the "gyroscope effect." If the spacecraft rotates with angular frequency Ω, the bearings in the turboexpander must have sufficient load capacity to support the torque τ on the shaft. For the turboexpander shaft spinning at 9000 rev/s, its angular momentum M_s is 1.8×10^{-4} kg–m^2/s. Assuming the bearings are separated by a distance L_s equal to 2.06 cm, the allowable spin of the spacecraft about an axis perpendicular to the shaft is 0.9 rev/s (54 rpm). If a mission is chosen for the cryocooler in which the spacecraft must spin faster

Creare

than about 0.5 rev/s, it may be necessary to orient the turboexpander such that its shaft is aligned with the spin axis of the spacecraft, thereby eliminating the gyroscopic force that might otherwise develop.

Environmental Vibrations. Periodic spacecraft vibrations are typically described by a frequency and acceleration level. The bearings of the turboexpander will behave like a spring–damper isolation system. For vibrations below the natural frequency, the vibrations will be transmitted to the shaft with little attenuation. For vibration frequencies higher than $2^{0.5}$ times the resonant frequency, the amplitude of the vibration transmitted to the shaft will be attenuated. We are interested in preventing shaft displacement **relative** to the bearing bushing since this is the way contact would occur; therefore, a high transmissibility is desirable. (This is contrary to the design philosophy of vibration isolation systems, for which the **absolute** motion of the isolated mass is minimized.)

Table 5.1 lists the periodic disturbances that have been measured on the Space Shuttle (Grodsinsky and Brown, 1989). In general, the disturbances are low frequency (below the calculated bearing resonant frequency of about 30 Hz). We therefore conclude that the bearing stiffness is adequate to protect the shaft from the vibratory disturbances expected on space-craft. If higher frequency disturbances are anticipated, a turboexpander housing mounting isolation system may be required for disturbances with amplitude greater than about 25 µm (0.001 in).

Table 5.1. SPACECRAFT PERIODIC DISTURBANCES		
a/g	Frequency (Hz)	Source
2×10^{-2}	9	Thruster fire (orbital)
2×10^{-3}	5 – 20	Crew motion
2×10^{-4}	17	Ku band antenna

Aerodynamic Loads. The geometry of the turbine end of the expander is such that multiple nozzles of a prescribed throat area introduce the gas to the turbine blades. The nozzles are symmetrically arranged about the shaft to minimize radial loading; however, due to manufacturing tolerances, the flow through each nozzle may not be identical. Assuming a

Creare

worst case situation regarding the location of nozzles with the highs and lows of dimensional tolerance, the resulting 2% flow imbalance would generate a force of about 6×10^{-4} N for typical turboexpander flows and conditions. The resulting displacement of the shaft in Meissner bearings would be approximately 6 μm (2.4×10^{-4} in). Since the turbine blade tip clearance would be about 5 times this value, there is little concern that aerodynamic imbalance would cause contact or significantly alter the performance of the turboexpander.

5.2 Thermodynamic Performance

Successful development of Meissner effect bearings for cryogenic turboexpanders can provide significant benefit to SDIO programs for cryogenic sensing through boosts in system efficiency (reduction in launch weight) and extensions of useful mission life. To quantify the potential benefit, consider the case of a three stage sensor cryocooler designed to carry a cold load at 10 K. We consider as a base case design the use of a cold turbine with gas bearings operating at radiator temperature, 300 K. Using state– of–the–art component performance estimates (eg., heat exchanger effectiveness = 0.98, motor and inverter efficiencies = 0.90) and optimizing system design around those figures, we computed the net cycle input power using the three–stage cryocooler design shown in Figure 5.1.

To assess the benefit of Meissner bearings, we then recalculated the cycle performance assuming the cold turbine bearings are at cryogenic temperatures, thereby decreasing the heat leak to the turbine. To do this, we make the following assumptions.

- The turbine power extracted from the cold stream is dumped via the brake circuit to the warmest load at 70 – 80 K.

- The heat leak to the turbine is reduced due to both the decreased axial temperature gradient along the shaft and the decreased thermal conductivity of the shaft material (titanium) at cryogenic temperatures.

We studied the improvement afforded by Meissner bearings for cold loads between 1 and 10 watts, and for a bearing temperature of 75 K. The cases studied are summarizing in the Table 5.2.

Figure 5.2 displays the sensitivity of cycle input power to cold load cooling power for optimized system designs. The attendant reduction in cold turbine heat leak is responsible for
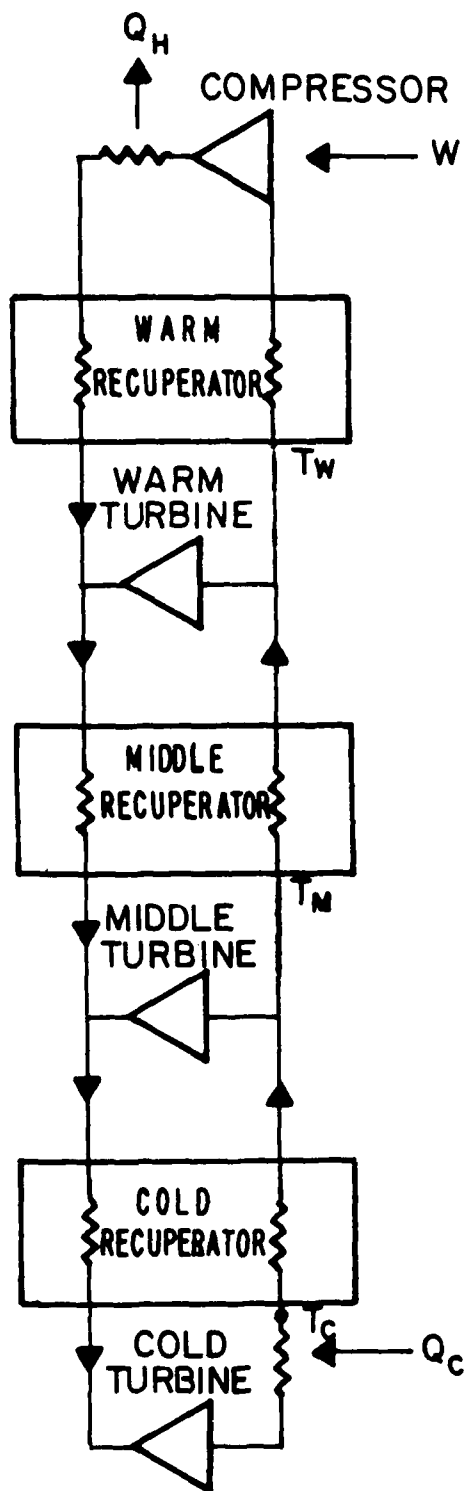
Figure 5.1. THREE STAGE CRYOCOOLER USED TO COMPARE CYCLE PERFORMANCE FOR MEISSNER AND GAS BEARINGS IN COLD TURBOEXPANDER
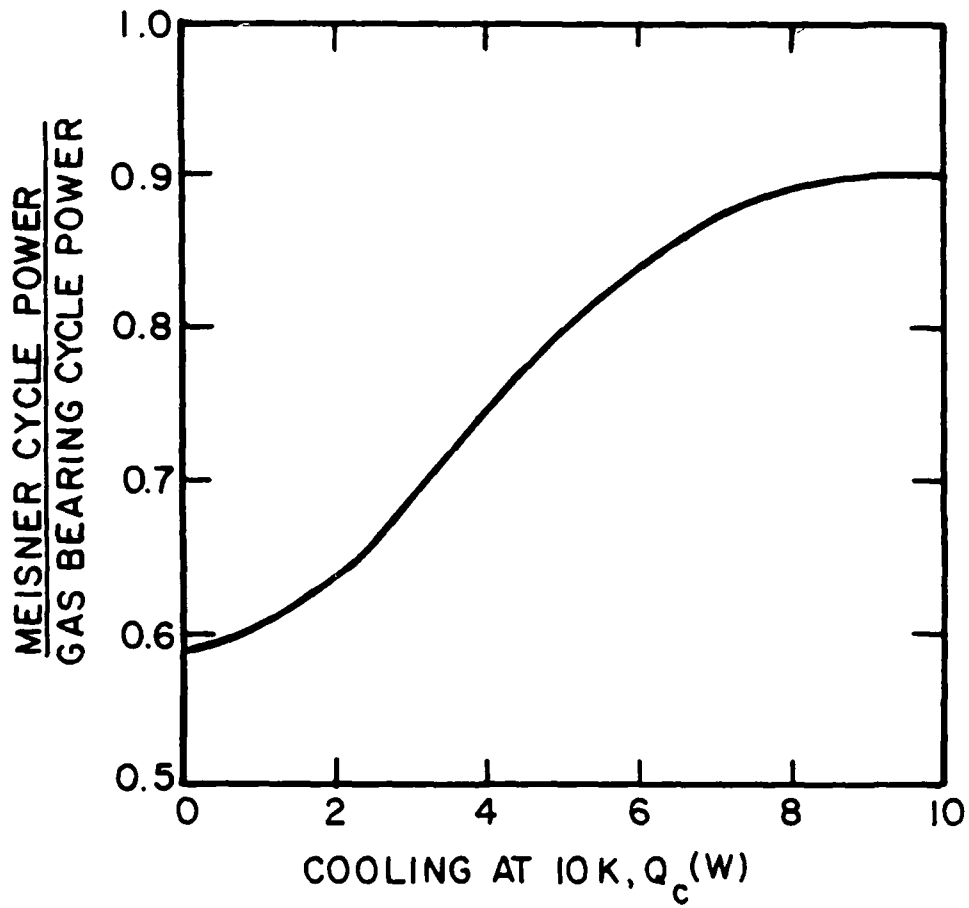
Figure 5.2. COMPARISON OF MEISSNER BEARING TURBOEXPANDER AND GAS BEARING TURBOEXPANDER CYCLE INPUT POWERS

reare

Table 5.2. SUMMARY OF CRYOCOOLER CYCLES STUDIED		
Parameter	Variable	Value
Cold Load	Q_L	1 – 10 W
Cold Temperature	T_L	10 K
Middle Temperature	T_M	30 W
Warm Temperature	T_W	70 – 80 K

the improvement in overall cycle efficiency. For each case, we reoptimized the system design to take maximum overall benefit from cold stage improvements, and recomputed the cycle input power. Failure to reoptimize the system design would tend to overstate the benefit achievable by using Meissner bearing in the cold stage. We see in Figure 5.2 that for cold loads between 1 and 10 watts, the reduction in cycle input power is between 10 and 40%, with the largest benefit for the smallest cooling loads. Since overall system weight is almost directly proportional to input power for such a system, we see that Meissner bearings have the potential to reduce the system launch weight by 40% for cold stage cooling loads on the order of 1 W. We therefore conclude that the thermodynamic performance of a system employing Meissner bearings in the cold turboexpander significantly exceeds that of the corresponding system employing self–acting gas bearings.

5.3 Reliability

Like active magnetic bearings and gas bearings, Meissner bearings will operate for indefinite periods of time because the elimination of solid–solid contact results in no wear of the bearings. The primary reliability issues are therefore related to the bearing behavior when not superconducting (not levitating the shaft).

The first step to achieving high reliability is to ensure the turboexpander is not operated when the bearings are not superconducting. This can be accomplished by incorporating a temperature sensor embedded in or close to the superconductor bushing which provides a signal to the appropriate controller.

Creare

A means must also be provided to prevent shaft motion relative to the bushing when not superconducting. This can be accomplished by an electromagnetic "lock" on the shaft. When energized, the electromagnet would attract the shaft towards the bearing surface and hold it motionless relative to the bushing. The strength of the electromagnet would be strong enough to ensure the immobility of the shaft, but weak enough so that no damage was done to the bearing when the lock is first turned on. The controlled damping coils discussed in Section 2, could be energized to perform this function, since they are not needed when the shaft is not running.

An area to be addressed in Phase II is related to material degradation. YBaCuO is known to degrade in the presence of oxygen, water and carbon dioxide. The turboexpander will typically operate in ultrapure helium, which should not degrade its superconducting properties. The YBaCuO material will also degrade when in contact with most metals, but does not react with silver. Silver can therefore be used as a protective coating where metal contact is required. The degradation of the superconductor's levitating and physical properties will be experimentally quantified in Phase II.

Based on the no–wear characteristic of the Meissner bearing, as well as our assessment of material degradation and start/stop cycling issues, we believe that the Meissner bearing will be a highly reliable device. In Phase II, a task will be devoted to demonstrating this high reliable via an endurance rig.

5.4 Manufacturability

Our turboexpander with Meissner bearings is conceptually similar to the turbo-expanders employing self–acting gas bearings that we have previously developed. The geometry of the superconductor is annular, which is available from suppliers of bulk super-conducting materials. The dimensional tolerances required of the superconductor can be achieved by the modeling process commonly used to form bulk superconductors. Based on the availability of the ceramic superconductors and the adequacy of current fabrication techniques, we conclude that the fabrication of a turboexpander employing Meissner bearings is completely feasible. In fact, Meissner bearings are much simpler than tilting pad gas bearings to fabricate.

Creare

6 CONCLUSIONS OF PHASE I WORK

In Phase I, we have performed a study to evaluate the feasibility of employing Meissner bearings in a cryogenic turbomachine. The specific technical objectives of the Phase I effort were to:

- Determine the performance characteristics of Meissner journal bearings.

- Establish suitable fabrication techniques and candidate materials.

- Design a Meissner bearing suitable for incorporation into a cryogenic turbomachine.

The first task to achieving these objectives was to analyze the dynamic performance of Meissner bearings. We extended the state–of–the–art developed for levitation of a magnet above a Type II superconductor to our bearing geometry. Based on this analysis, we conclude that a bearing stiffness of about 50 N/m can be achieved for a bearing for a 0.318 cm (1/8 in) shaft using ceramic superconductors such as YBaCuO.

In the next task, we assessed material properties and fabrication techniques. Since for our application, we are interested in superconductors with critical temperatures T_c greater than about 70 K, we concentrated on the yttrium, bismuth, and thallium ceramic superconductors. Our analytical model predicts that stiffness is proportional to B_{c1} for materials with weak flux pinning. The use of yttrium superconductor was therefore found to maximize the levitation forces obtainable because for superconductors with $T_c > 70$ K, it has the greatest value of B_{c1} (~ 0.01 T). Its mechanical properties (elastic modulus, thermal expansion, strain–to–failure) were also determined to be sufficient for incorporation into our bearing. Current fabrication can be employed to produce a superconductor of the desired shape within a dimensional tolerance of 25 μm (0.001 in).

Based on the results of the first two tasks, we designed a turboexpander incorporating Meissner journal bearings. The design is similar to that of previous turboexpanders employing self–acting gas bearings. The turboexpander is expected to produce about 5 W of cooling at about 10 K, depending on the cycle in which it is used. It incorporates a 0.318 cm (1/8 in) shaft that spins at 9000 rev/s. The bearing temperature, however, is designed to be about 75 K

Creare

as compared to the 300 K required by self-acting gas bearings. As a result, the heat leak down the shaft is reduced, with a corresponding increase in cycle efficiency.

Based on the work performed in the previously described tasks, the overall technical feasibility of the Meissner bearing concept was next assessed. The 2.5 gram load capacity of the bearings was determined to be sufficient to withstand spacecraft accelerations up to 2.0g, and aerodynamic loads caused by conservatively estimated flow imbalance in the turbine. The thermodynamic performance of a three-stage cryocooler employing Meissner bearing in the coldest turbine fared favorably with a similar cycle employing conventional turboexpanders with self-acting gas bearings in that a 40% reduction in cycle input power results because of the reduced heat leak afforded by operating the bearings at cryogenic temperatures. The Meissner bearings who also determined to be highly reliable due to their non-contact mode of operation. This contrasts self-acting bearings, which generate their levitation forces only when the shaft is spinning at a sufficiently high speed. One needs only to ensure that the shaft is spun only when the superconducting material is actually superconducting, i.e., below its critical temperature.

In summary, this Phase I project has demonstrated the feasibility and potential performance gain afforded by the incorporation of Meissner bearings into a cryogenic turboexpander. Based on this work, we are confident that Meissner bearings for cryogenic turbomachines can be successfully implemented, and we therefore strongly recommend its continued development.

@reare

7 REFERENCES

Bender, C.M. and Orszag, S.A.; Advanced Mathematical Methods for Scientists and Engineers; New York, NY, McGraw–Hill, 1978.

Grassam, N.S. and Powell, J.W.; Gas Lubricated Bearings; London, England, Butterworth and Co., 1964.

Green, M.A.; *High T_c Superconductor and Superconducting Magnets*; in Superconductivity Applications and Developments, MD–V11, ASME, New York, 1988.

Green, A.E. and Naghdi, P.M.; *Aspects of the Second Law of Thermodynamics in the Presence of Electromagnetic Effects*; Quart. J. Mech. Appl. Math., V37, 1984, pp. 179–193.

Grodsinsky, C.M. and Brown, G.V.; *Low Frequency Vibration Isolation Technology for Microgravity Space Experiments*; to be presented at the 12th Biennial Conference on Mechanical Vibration and Noise, Montreal, Canada, Sept. 17 – 20, 1989.

Harter, W.G., Hermann, A.M. and Sheng, Z.Z.; *Levitation Effects Involving High T_c Thallium Based Superconductors*; Appl. Phys. Lett., V53(12), Sept. 1988, pp. 1119–1121.

Hellman, F., Gyorgy, E. M., Johnson, D.W., O'Bryan, H.M. and Sherwood, R.C.; *Levitation of a Magnet Over a Flat Type II Superconductor*; J. Appl. Phys., V63, 1988, pp. 447–450.

Kumakura, H., Takahashi, K., Dietderich, D.R., Togano, K. and Maede, H.; *Superconductivity and Magnetic Properties of High T_c Bi-Sr-Ca-Cu-O Superconductors*; Appl. Phys. Lett., V52, 1988, pp. 2064–2065.

Kumakura, H., Togano, K., Fukutomi, M., Uehara, M. and Tachikawa, K.; *Magnetiztion Measurements in Y-Ba-Cu-O Compound System*; Jap. J. Appl. Phys., V26, 1987, pp. L655–L656.

Laquer, H.L.; *High Temperature Superconductivity: What, Why, Where and How*; Proceedings 23rd Intersociety Energy Conversion Engineering Conf., Denver, Colorado, 1988, pp. 493–499.

Lee, W.Y., Lee, V.Y., Salem, J., Huang, T.C., Savoy, R., Bullock, D.C. and Parkin, S.S.P.; *Superconducting T1-Ca-Ba-Cu-O Thin Films with Zero Resistance at Temperatures up to 120 K*; Appl. Phys. Lett., V53, 1988, pp. 329–331.

Marshall, D.B., et al.; *Flux Penetration in High-T_c Superconductors: Implications for Magnetic Suspension and Shielding*; Appl. Phys. A, V48, 1989, pp. 87–91.

Moon, F., Hull, J.R. and Berry, G.F.; *Superconductivity: As Temperatures Rise, So Do Demands on MEs*; Mechanical Engineering, V110, 1988, pp. 60–68.

Moon, F.C., Yanoviak, M.M. and Ware, R.; *Hysteretic Levitation Forces in Superconducting Ceramics*; Appl. Phys. Lett., V52(18), May 2, 1988, p. 1534.

Creare

Murphy D.W., Johnson, D.W., Jin, S. and Howard, R.E.; *Processing Techniques for the 93 K Superconductor Ba$_2$ Y Cu$_3$ O$_7$*; Science, V241, 1988, pp. 922–930.

Simon, I.; *Forces Acting on Superconductors in Magnetic Fields*; J. Applied Physics, V24(1), Jan. 1953, p. 19.

Tinkham, M.; Introduction to Superconductivity, New York, NY, McGraw–Hill, 1975.

Uchida, S., et al.; *High-T$_c$ Superconductivity of La-Ba(Sr)-Cu Oxides*; IV Critical Magnetic Fields, Jap. J. Appl. Phys., V26, 1987, pp. L196–L197.

Williams, R. and Matey, J.R.; *Equilibrium of a Magnet Floating Avove a Superconducting Disk*; Appl. Phys. Lett., V52(9), Feb. 29, 1988, p. 751.